GREM1 Negatively Regulates Osteo-/Dentinogenic Differentiation of Dental Pulp Stem Cells via Association with YWHAH

Shu DIAO[1,2], Xiao HAN[1], Wei Long YE[1], Chen ZHANG[1], Dong Mei YANG[2], Zhi Peng FAN[1,3], Song Lin WANG[1,3]

Objective: *To investigate the biological regulatory function of Gremlin1 (GREM1) and tyrosine 3-monooxygenase/tryptophan 5-monooxygenase activation protein eta (YWHAH) in dental pulp stem cells (DPSCs), and determine the underlying molecular mechanism involved.*
Methods: *Alkaline phosphatase (ALP) activity, alizarin red staining, scratch migration assays and in vitro and in vivo osteo-/dentinogenic marker detection of bone-like tissue generation in nude mice were used to assess osteo-/dentinogenic differentiation. Coimmunoprecipitation and polypeptide microarray assays were employed to detect the molecular mechanisms involved.*
Results: *The data revealed that knockdown of GREM1 promoted ALP activity, mineralisation in vitro and the expression of osteo-/dentinogenic differentiation markers and enhanced osteo-/dentinogenesis of DPSCs in vivo. GREM1 bound to YWHAH in DPSCs, and the binding site was also identified. Knockdown of YWHAH suppressed the osteo-/dentinogenesis of DPSCs in vitro, and overexpression of YWHAH promoted the osteo-/dentinogenesis of DPSCs in vitro and in vivo.*
Conclusion: *Taken together, the findings highlight the critical roles of GREM1-YWHAH in the osteo-/dentinogenesis of DPSCs.*
Keywords: *dental pulp stem cells, Gremlin1, tooth regeneration, YWHAH*
Chin J Dent Res 2024;27(3):203–213; doi: 10.3290/j.cjdr.b5698390

1 Salivary Gland Disease Center and Beijing Key Laboratory of Tooth Regeneration and Function Reconstruction, Beijing Laboratory of Oral Health and Beijing Stomatological Hospital, Capital Medical University, Beijing, P.R. China.
2 Department of Pediatric Dentistry, Capital Medical University School of Stomatology, Beijing, P.R. China.
3 Research Unit of Tooth Development and Regeneration, Chinese Academy of Medical Sciences, Beijing, P.R. China.

Corresponding authors: Prof Zhi Peng FAN, Capital Medical University School of Stomatology, No. 4 Tian Tan Xi Li, DongCheng District, Beijing 100050, P.R. China. Tel: 86-10-57099114. Email: zpfan@ccmu.edu.cn; Prof Song Ling WANG, Capital Medical University, No.10 You An Men Wai Xi Tou Tiao, FengTai District, Beijing 100069, P.R. China. Tel: 86-10-83911708. Email: slwang@ccmu.edu.cn.

This work was supported by grants from the National Natural Science Foundation of China (82130028 to ZPF), the National Natural Science Foundation of China (92049201, 82030031, 81991504, 92149301, L2224038 and 82001067), the Beijing Municipal Government grant (Beijing Laboratory of Oral Health, PXM2021-014226-000041), the Innovation Research Team Project of Beijing Stomatological Hospital, Capital Medical University (CXTD202201), the Beijing Advanced Innovation Center for Big Data-based Precision Medicine (PXM2021_014226_000026), the Beijing Municipal Government (Beijing Scholar Program, PXM2020_014226_000005 and PXM2021_014226_000020), the National Key Research and development Program (2022YFA1104401) and the National Sciences Foundation of China (81800923 to SD).

Stem cell–mediated tooth regeneration is an ideal therapy for tooth loss but still presents many problems, such as limited seed cells and poor efficacy.[1,2] In tooth tissue, stem cells, growth factors and the extracellular matrix (ECM) in the niche and their multiple interactions determine tooth development, eruption and biological basis for the formation of pulp dentine and so on. However, due to being limited by the current methods, the niche cannot be maintained when mesenchymal stem cells (MSCs) are isolated and cultured in vitro. Disruption of the niche may impede MSC-mediated tooth regeneration.[3-5] The stem cell niche plays a key role in homeostasis and tissue regeneration.

From the perspective of the stem cell microenvironment, previous studies conducted by the present authors[6,7] revealed that bone morphogenetic proteins (BMPs) are downregulated in stem cells from the apical papilla (SCAPs) compared with the tissues from the apical papilla, but the antagonist of bone morphogenetic protein- Gremlin1 (GREM1) is upregulated. In vitro experiments showed that BMP6 could significantly enhance the proliferation and differentiation potential

of SCAPs, and that BMP2, BMP6 and BMP7 are negatively regulated by GREM1, suggesting that the GREM1-BMP signalling pathway may play an important role in regulating the function of stem cells.[6,7]

GREM1 belongs to the DNA family of secreted BMP antagonists. GREM1 is involved in bone development, and Grem1 mutant mice develop severe limb skeletal deformities.[8,9] As an endogenous antagonist of BMP, GREM1 not only binds to extracellular BMP but also prevents the secretion of BMP through intracellular BMP and GREM1 interactions and effectively inhibits its activity.[10] Studies have confirmed that Grem1 blocks the classical BMP signalling pathway by inhibiting the phosphorylation of smad1/5/8, but can also directly regulate p38, ERK and JNK.[11] However, until recently, the interaction between BMP signalling and GREM1 in MSCs has been unclear. A previous study revealed that GREM1 can bind to tyrosine 3-monooxygenase/tryptophan 5-monooxygenase activation protein eta (YWHAH),[12] a member of the 14-3-3 gene family. The 14-3-3 protein family is a group of highly conserved acidic proteins that are highly expressed in nervous tissues; it interacts with more than 100 proteins that are critical for many cellular physiological processes, such as signalling, cell growth, division, adhesion, derivatives and apoptosis, and thus plays an important role in cell proliferation and transformation.[13-15] These studies indicated that YWHAH might be a downstream gene of GREM1, and regulate BMP2, BMP6 and BMP7 and stem cell function[16,17]; however their function and molecular mechanism are not clear. In this study, the present authors investigated the biological regulatory function of GREM1 in DPSCs, and the underlying molecular mechanism to explain how GREM1/YWHAH regulate BMPs in DPSCs.

Materials and methods

Cell culture

With the approval of the Beijing Stomatology Hospital, School of Stomatology, Capital Medical University (CMUSH-IRB-KJ-PJ-2023-28), human impacted third molars were collected from 10 healthy patients. The pulp tissues were treated aseptically and washed with solutions of phosphate-buffered saline (PBS). DPSCs were isolated and cultured as previously described. Briefly cells were grown in a humidified atmosphere of 5% CO_2 at 37°C, and the medium was changed every 3 days.

Plasmids and viruses

Plasmids were produced using standard methods, and enzyme digestion, sequencing or both confirmed the structures of all plasmids. Human full-length YWHAH cDNA with an HA tag was generated via standard gene synthesis. This fragment (HA-YWHAH) was inserted into the PQCXIN plasmid between the AgeI and BamH1 restriction sites. GREM1 shRNA, YWHAH shRNA and control shRNA were purchased from Genepharma (Suzhou, China). DPSCs were seeded into plates overnight growth and transfected for 12 hours with the virus using polybrene (Sigma Aldrich, St. Louis, MO, USA). After 48 hours of transfection, the cells were selected in the presence of an appropriate antibiotic. The sequences of the shRNAs used were follows: LV3 shRNA (Consh), 5'-TTCTCCGAACGTGTCACGTTT-3'; GREM1 shRNA (GREM1-sh), 5'-GCAAGCCC AAGAAATTCACTA-3'. NC shRNA (Consh), 5'-CCATGATTCCTTCATATTTGC-3'; YWHAH shRNA (YWHAH-sh), 5'-GAGCCGACACGGGTTAGGATCC-3'.

Cell ALP activity assay and alizarin red staining

DPSCs were grown in mineralisation-inducing medium using a Stem Pro Osteogenesis Differentiation Kit (Invitrogen, Carlsbad, CA, USA). Cells were cultured for 5 days, and the ALP activity assay was performed with an ALP kit according to the manufacturer's protocol (Sigma Aldrich) and normalised based on protein concentrations. The protein concentration was quantitatively determined using Bio-Rad protein assay solution (Bio-Rad Laboratories, Hercules, CA, USA). To detect mineralisation, the cells were induced for 2 weeks, fixed with 70% ethanol and stained with 2% alizarin red (Sigma Aldrich). To quantitatively determine the calcium mineral content, alizarin red was destained with 10% cetylpyridinium chloride in 10 mM sodium phosphate for 60 minutes at room temperature. The concentration was determined by absorbance measurement at 562 nm on a multiplate reader using a standard calcium curve in the same solution. The final calcium level in each group was normalised to the total protein concentration prepared from a duplicate plate.[18]

Reverse transcriptase polymerase chain reaction (RT-PCR) and real-time RT-PCR

Total RNA was isolated from DPSCs with TRIzol reagent (Invitrogen). We synthesised cDNA from 2 µg aliquots of RNA, random hexamers or oligo (dT) and reverse transcriptase, according to the manufacturer's protocol (Invitrogen). Real-time PCR was performed with a Quanti-

Tect SYBR Green PCR Kit (Qiagen, Hilden, Germany) and an Icycler iQ Multicolor Real-time PCR Detection System (Bio-Rad Laboratories). The primers for specific genes are shown in Table S1 and the PCR conditions are presented in Table S2 (both provided on request).

Scratch migration assays

A scratch-simulated wound migration assay was implemented to assess the function of MSC migration. Upon reaching 80% confluence, the cells were digested with 0.25% trypsin-ethylenediaminetetraacetic acid (EDTA) (Gibco, Life Technologies, Carlsbad, CA, USA), seeded onto six-well plates at a density of 2×10^5 cells/well and allowed to grow to close to 95% confluence. The cells were grown in DMEM supplemented with alpha modified Eagle medium (Invitrogen) without foetal bovine serum (FBS; Invitrogen). After culturing for 24 hours, a cross scratch was made in the cell layer along the diameter of the well with a 200-µl pipette tip (Axygen, Corning, NY, USA), and the cells were grown in fresh culture media. Images from the same view were taken under a microscope at baseline (0 hours), 24 hours and 48 hours after wounding to determine the extent of wound closure. Image-Pro1.49v (National Institutes of Health, Bethesda, MD, USA) was used to measure the void area (VA) and the height and relative width were evaluated (area% = VA/height) in each group.

Western blot

Total proteins were extracted from DPSCs, and SDS polyacrylamide gel electrophoresis was performed as described previously. The primary antibodies used in this study were against GREM1 (cat no. G4672; Sigma Aldrich), YWHAH (cat no. F1804; Sigma Aldrich) and GAPDH (cat. no. G8795, Sigma Aldrich).

Coimmunoprecipitation (Co-IP) assay

DPSCs were lysed with IP lysis buffer (Invitrogen). The cell lysates were incubated with a specific primary antibody and protein A/G Sepharose (Santa Cruz Biotechnology, Dallas, TX, USA) was added overnight at 4°C. After washing, the immunoprecipitated complex was treated with either RNase A or RNase inhibitor (Sigma Aldrich) for 5 minutes at 37°C. The cells were resuspended in SDS-PAGE loading buffer for Western blot analysis using the corresponding antibodies. The primary antibodies used in this study were against GREM1 (cat no. G4672; Sigma Aldrich), YWHAH (cat no. G7633; Sigma Aldrich) and GAPDH (cat. no. G8795, Sigma Aldrich).

Peptide microarray

Polypeptide chip sealing

After the array membrane was activated, sealing solution was added and the membrane was sealed for 4 hours with shaking at room temperature.

Reactive protein labelling

A biotin labelling kit (EZ-LINK^{TM}NHS-PEG$_4$-BIOTIN, PIECE, LOT$_{\#tg}$263646) was used to label the GREM1-isoform1 protein with a biotin reminder. The binding of polypeptide chip was incubated with reactive protein, and the biotin-labelled GREM1-isoform1 protein was diluted with sealing solution and incubated with the array. The experimental group was incubated with 10 ml reaction solution at a concentration of 4 µg/ml, and the control group chip was incubated with sealing fluid. The membrane was shaken overnight at 4°C, the diaphragm was removed, and the membrane was washed with TBST five times.

Polypeptide chip and HRP-labelled secondary antibody incubation

The membrane was washed with high-sensitivity streptavidin-HRP (Pierce CA#:21130) and diluted with sealing solution. After 1:8,000, the membranes in the experimental group and control group were incubated with 5 ml each, shaken at room temperature for 2 hours, and then washed five times.

Colour development

TotalLab image analysis software (TotalLab, Gosforth, UK) was used to analyse the optical density values of colour rendering points for imaging images. The "Spot Edge Average" algorithm reads the colour rendering values of all peptide segments and sets the colour point light on the film. The highest density value is 100%, with reference to the surrounding background values of each colour developing point, and the optical density values of other points are calculated as the percentage values of the optical density values of the point. The possible binding sites and fragment sequences of GREM1 and YWHAH were obtained through bioinformatics comparative analysis.

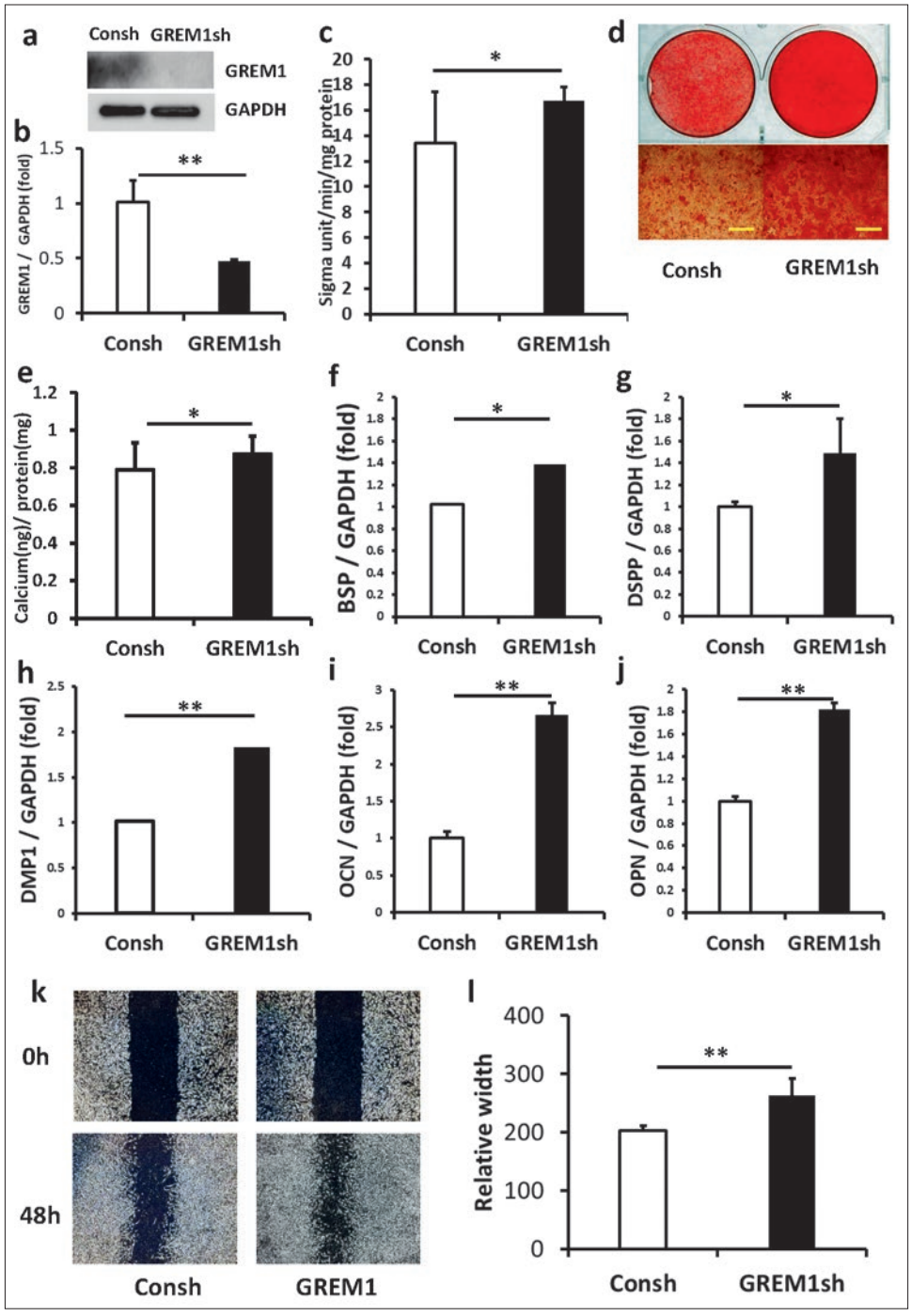

Fig 1a to l Knockdown of GREM1 promoted the osteo-/dentinogenic differentiation of DPSCs in vitro. Western blot analysis of GREM1 expression **(a)**. Real-time RT-PCR showed the knockdown efficiency of GREM1 in DPSCs **(b)**. ALP activity assay **(c)**. Alizarin red staining **(d)**. Quantitative calcium analysis **(e)**. The expression of DSPP **(f)**, DMP1 **(g)**, BSP **(h)**, OPN **(i)** and OCN **(j)** was detected by real-time RT-PCR at 14 days after induction. The results of the scratch-simulated wound migration assay **(k and l)**. GAPDH was used as an internal control. A Student *t* test was performed to determine statistical significance. All error bars represent the standard deviation (n = 6). $*P \leq 0.05$, $**P \leq 0.01$.

Nude mouse transplantation with haematoxylin-eosin (HE) staining and immunohistochemical staining

A total of 2.0×10^6 DPSCs were mixed with MC (Engineering Research Center for Biomaterials, Tsinghua University, Beijing, China) at 37°C for 2 hours, and then the mixture was subcutaneously transplanted into the backs of nude mice (10-week-old females, nu/nu). After 8 weeks, the subcutaneous transplanted tissues were collected, fixed with 10% formalin and decalcified in 10% EDTA. The tissues were stained with haematoxylin-eosin (HE). Image-Pro Plus software (Media Cybernetics, Rockville, MD, USA) was used to calculate the area of bone/dentine-like tissue. Immunohistochemical

staining was performed as described previously.[18] The primary antibodies used were DSPP (cat no. bs10316R, Bioss, China) and BSP (cat no. bs2668R, Bioss, China). The present research was carried out in accordance with the animal experiment regulations.

Statistical analysis

Statistical calculations were implemented using SPSS 10.0 statistical software (SPSS, Chicago, IL, USA). Statistical significance was analysed using a Student *t* test; $P \leq 0.05$ was defined as statistically significant.

Results

Knockdown of GREM1 promoted the osteo/dentinogenic differentiation of DPSCs in vitro and in vivo

First, we constructed a short hairpin RNA (shRNA) to inhibit GREM1 expression and introduced it into DPSCs via lentiviral infection. Infected cells were selected with 2 μg/ml puromycin for 3 days, and the efficiency of GREM1 knockdown was confirmed by real-time RT-PCR and western blotting (Fig 1a and b). After the cells were cultured in osteogenic induction medium, we evaluated their osteogenic differentiation potential. After osteogenic induction for 5 days, the ALP activity in GREM1 knockdown DPSCs was greater than that in control DPSCs (Fig 1c). Alizarin red staining and quantitative calcium measurements showed that GREM1 depletion in DPSCs promoted mineralisation compared to that in control DPSCs (Fig 1d and e). The real-time RT-PCR results showed that GREM1 depletion in DPSCs enhanced BSP, DSPP, DMP1, OCN and OPN expression on day 14 after induction (Fig 1f to j). Then, the scratch-simulated wound migration assay results showed that GREM1 knockdown promoted the migration of DPSCs at 48 hours (Fig 1k and l). Finally, control DPSCs and GREM1 knockdown DPSCs were transplanted subcutaneously into nude mice. We discovered that GREM1 knockdown DPSCs formed more bone/dentine-like tissues (Fig 2a and b). Moreover, immunohistochemical staining and quantitative analysis revealed that DSPP and BSP expression were greater in GREM1 knockdown DPSCs than in control DPSCs (Fig 2c to f).

GREM1/YWHAH can regulate BMP2, BMP6 and BMP7 expression

We used real-time RT-PCR to detect BMP expression. The results showed that GREM1 depletion in DPSCs enhanced BMP2, BMP6 and BMP7 expression (Fig 3a to c). Knocking down YWHAH in DPSCs suppressed the expression of BMP2, BMP6 and BMP7 (Fig 3d to f). Overexpression of YWHAH promoted the expression of BMP2, BMP6 and BMP7 (Fig 3g to i).

GREM1 can bind to YWHAH in DPSCs

We examined the association of GREM1 with YWHAH in DPSCs. Co-IP showed that the formation of GREM1-YWHAH protein complexes increased with HA-GREM1 overexpression in DPSCs (Fig 4a). In addition, depletion of GREM1 decreased the formation of GREM1-YWHAH protein complexes in DPSCs (Fig 4b). Co-IP results showed that the overexpression of YWHAH promoted the association of GREM1 and YWHAH in DPSCs (Fig 4c), and knocking down of YWHAH in DPSCs suppressed this association (Fig 4d). Furthermore, polypeptide microarray results showed that the polypeptide array derived from the YWHAH protein sequence can bind to the reactive protein GREM1-isoform1 protein, and the protein binding polypeptide points 29, 46 and 47 have obvious colour rendering effects (Fig 4e). Taken together, these results indicate that GREM1 binds to YWHAH. The effective binding sites were- L R D N L T L W T S D Q Q D E and -T L W T S D Q Q D E E A G E G.

Knockdown of YWHAH suppressed the osteo-/dentinogenesis of DPSCs in vitro

To verify the role of YWHAH in DPSCs osteo/dentinogenic differentiation, we constructed a short hairpin RNA (shRNA) to inhibit YWHAH expression and introduced it into DPSCs via lentiviral infection. Infected cells were selected with 2 μg/ml puromycin for 3 days, and the efficiency of YWHAH knockdown was confirmed by real-time RT-PCR and western blotting (Fig 5a and b). After osteogenic induction for 5 days, the ALP activity decreased in YWHAH knockdown DPSCs compared to control DPSCs (Fig 5c). Alizarin red staining and quantitative calcium measurements showed that YWHAH depletion in DPSCs suppressed mineralisation compared to that in control DPSCs (Fig 5d and e). The real-time RT-PCR results revealed that YWHAH depletion in DPSCs inhibited BSP, DSPP and DMP1 expression on day 14 after induction. There were no statistical differences in OCN and OPN (Fig 5f to j). Then, the scratch-simulated wound migration assay results showed that YWHAH knockdown repressed the migration ability of DPSCs at 48 hours (Fig 5k and l).

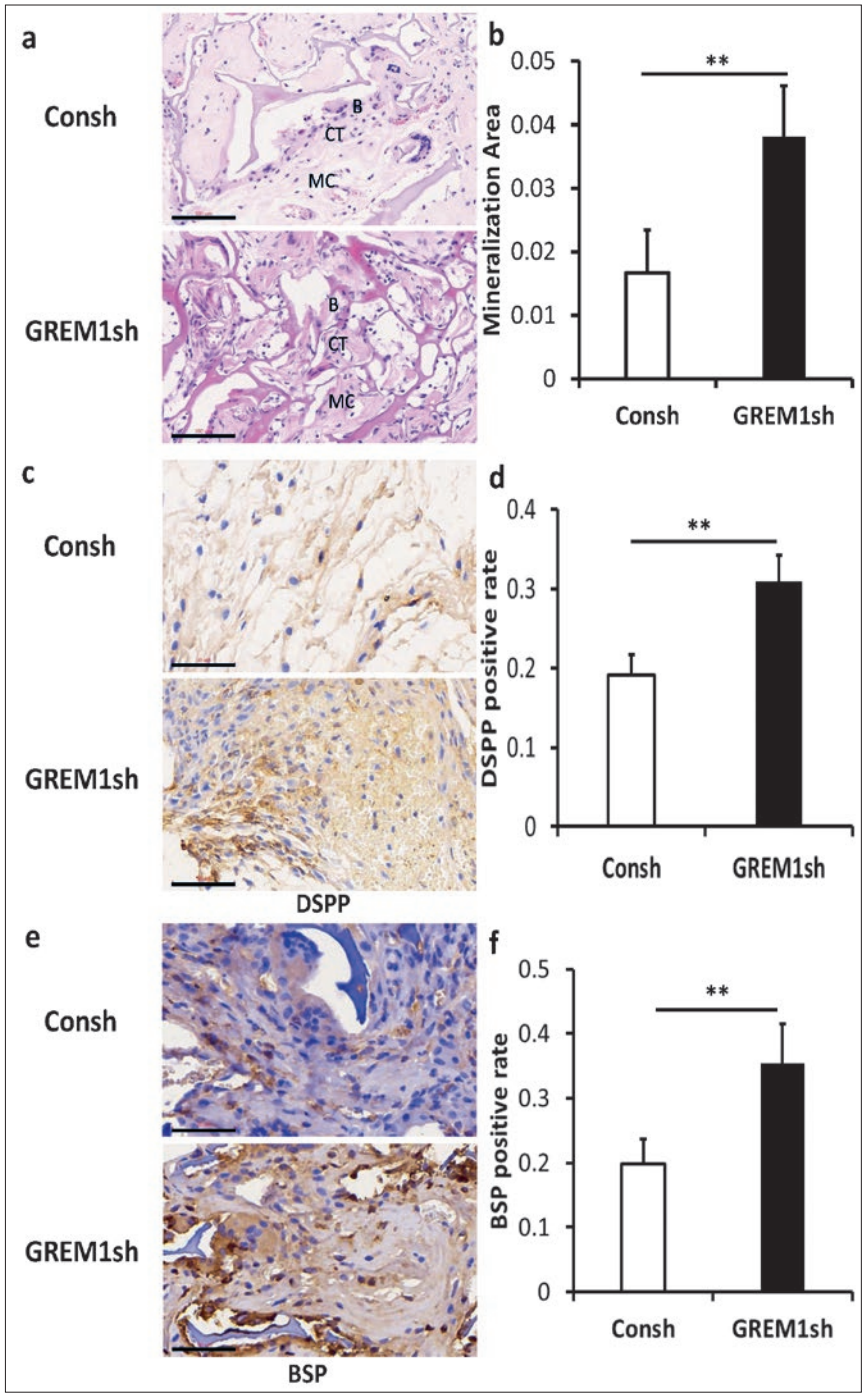

Fig 2a to f Knockdown of GREM1 promoted the osteo-/dentinogenic differentiation of DPSCs in vivo. HE staining results showing bone/dentine-like tissue formation. Scale bar 100 µm. B, bone/dentine-like tissues; CT, connective tissue; MC, mineral collagen **(a)**. Quantitative measurement of the HE staining results **(b)**. Immunohistochemical staining and quantitative analysis of DSPP **(c and d)**. Immunohistochemical staining and quantitative analysis of BSP. Scale bar 50 µm **(e and f)**. A Student *t* test was performed to determine statistical significance. All error bars represent the standard deviation (n = 6). *$P \leq 0.05$, **$P \leq 0.01$.

Overexpression of YWHAH promoted the osteo-/dentinogenesis of DPSCs in vitro and in vivo

The function of YWHAH in DPSCs was investigated by inserting the YWHAH sequence into a retroviral vector. Retroviral infected DPSCs were selected with 600 µg/ml G418 for 7 days, and western blot and real-time RT-PCR results confirmed the ectopic expression of YWHAH (Fig 6a and b). After osteogenic induction for 5 days, ALP activity increased in YWHAH overexpressing DPSCs compared to control DPSCs (Fig 6c). Alizarin red staining and quantitative calcium measurements revealed that compared with control DPSCs, YWHAH-overexpressing DPSCs promoted mineralisation (Fig 6d and e). The real-time RT-PCR results showed that YWHAH-overexpressing DPSCs exhibited increased BSP, DSPP, DMP1, OCN

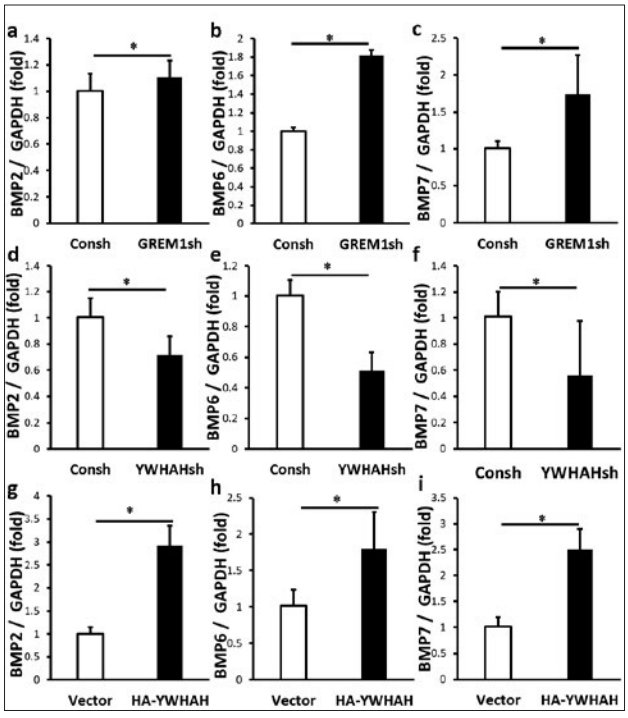

Fig 3a to i GREM1/YWHAH can regulate BMP2, BMP6 and BMP7 expression. The expression of BMP2 **(a)**, BMP6 **(b)** and BMP7 **(c)** was detected by real-time RT-PCR after knocking down GREM1 in DPSCs. The expression of BMP2 **(d)**, BMP6 **(e)** and BMP7 **(f)** was detected by real-time RT-PCR after YWHAH was knocked down in DPSCs. The expression of BMP2 **(g)**, BMP6 **(h)** and BMP7 **(i)** was detected by real-time RT-PCR after YWHAH was overexpressed in DPSCs.

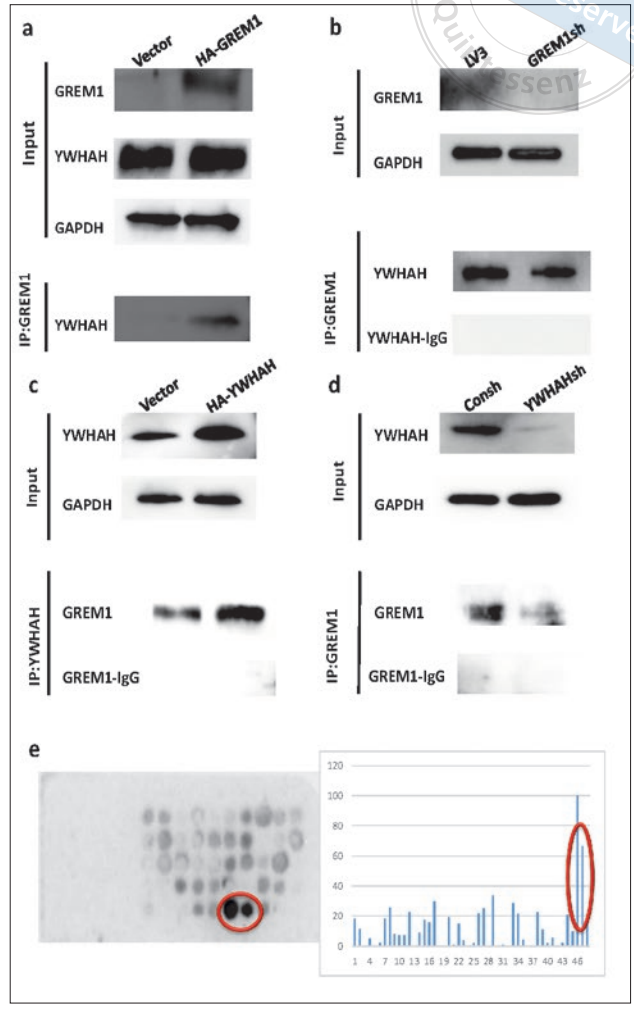

Fig 4a to e GREM1 binds to YWHAH in DPSCs. Western blot showing individual signals (input, 1% lysate) and coimmunoprecipitated protein complexes (IP, 99% lysate). Co-IP results showing more GREM1-YWHAH complexes in GREM1 overexpressing DPSCs **(a)**. Co-IP results showing fewer GREM1-YWHAH complexes in GREM1 silenced DPSCs **(b)**. Co-IP results showing more GREM1-YWHAH complexes in YWHAH overexpressing DPSCs **(c)**. Co-IP results showing fewer GREM1-YWHAH complexes in YWHAH silenced DPSCs **(d)**. There were binding sites in the polypeptide array experimental group. The grey value analysis software Total Lab TL100 showed that protein binding polypeptide points 29, 46 and 47 have obvious colour rendering effects **(e)**. GAPDH was used as an internal control.

and OPN expression on day 14 after induction (Fig 6f to j). The results of the scratch-simulated wound migration showed that YWHAH knockdown promoted the migration ability of DPSCs at 48 hours (Fig 6k and l). Finally, control DPSCs and YWHAH-overexpressing DPSCs were transplanted subcutaneously into nude mice. The present authors discovered that YWHAH-overexpressing DPSCs formed more bone/dentine-like tissues (Fig 7a and b). Moreover, immunohistochemical staining and quantitative analysis revealed that DSPP and BSP expression were greater in YWHAH-overexpressing DPSCs than in control DPSCs (Fig 7c to f).

Discussion

In tooth tissue engineering, using appropriate stem cells and scaffold materials, the present authors aimed to identify key target genes that affect the function of stem cells in the microenvironment, and apply genes to modify stem cells to improve their differentiation ability and enhance their performance, further improving the success rate of biological tooth root regeneration and shortening the regeneration cycle. GREM1, a member of the BMP antagonist family, plays an important role in regulating organogenesis, body patterning and tissue differentiation. Like other extracellular BMP antagonists, GREM1 contains a cysteine knot.[19-21] The role of GREM1 as a BMP antagonist has been identified in the kidney, limb development and lung branching morphogenesis.[22-24] A previous study conducted by the present authors found that GREM1 inhibited ADSC

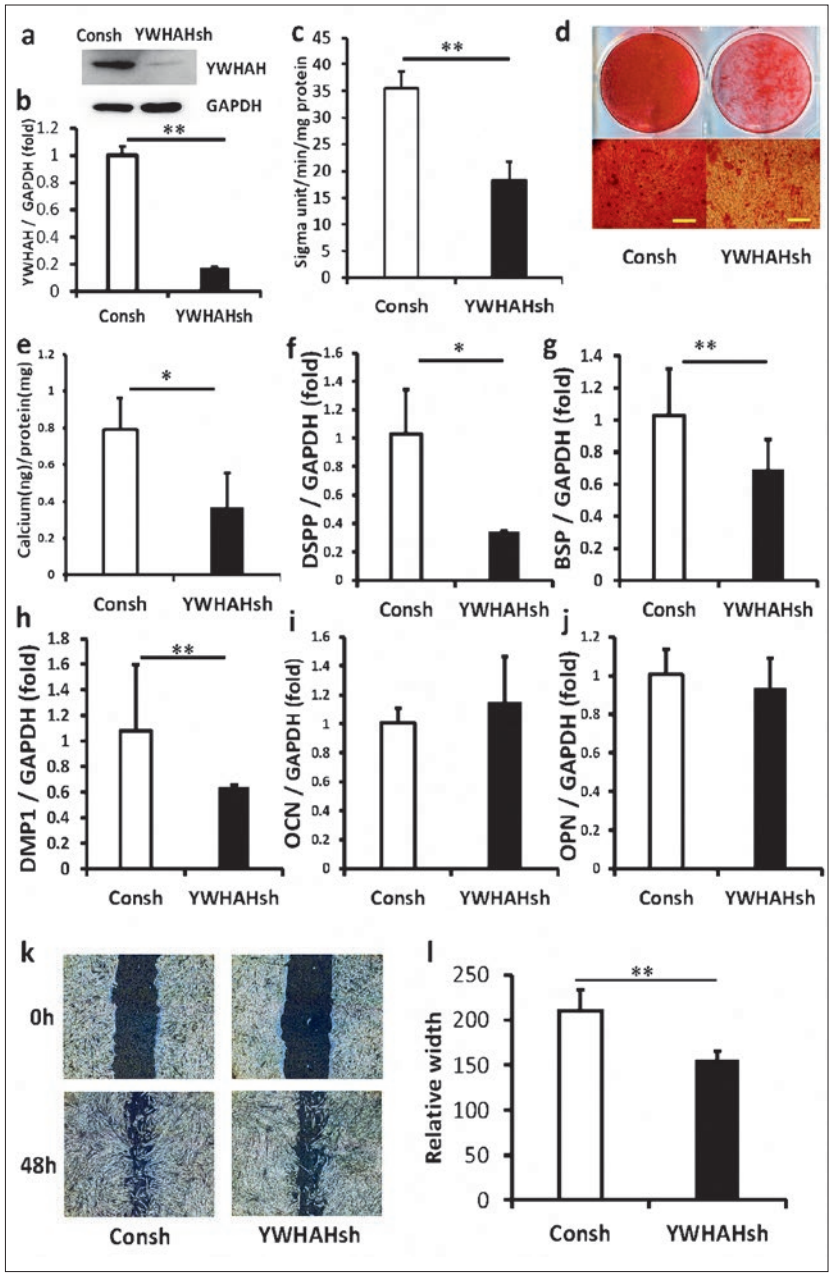

Fig 5a to l Knockdown of YWHAH suppressed the osteo-/dentinogenic differentiation of DPSCs in vitro. Western blot showing YWHAH expression **(a)**. Real-time RT-PCR showed the knockdown efficiency of YWHAH in DPSCs **(b)**. ALP activity assay **(c)**. Alizarin red staining **(d)**. Quantitative calcium analysis **(e)**. The expression of DSPP **(f)**, DMP1 **(g)** and BSP **(h)**, OPN **(i)** and OCN **(j)** was detected by real-time RT-PCR at 14 days after induction. The results of the scratch-simulated wound migration assay **(k and l)**. GAPDH was used as an internal control. A Student *t* test was performed to determine statistical significance. All error bars represent the standard deviation (n = 6). **P* ≤ 0.05, ***P* ≤ 0.01.

senescence and osteogenic differentiation potential and repressed BMP transcription. The present results provide new insights into the regulation of MSC functions and target the use of MSCs for bone regeneration. Thus, the authors conducted experiments to investigate the role of GREM1 in the osteo-/dentinogenic differentiation and migration of DPSCs in vitro and in vivo. First, alkaline phosphatase (ALP) activity, alizarin red staining and scratch migration assays showed that knockdown of GREM1 promoted osteo-/dentinogenic differentiation and migration of DPSCs in vitro. Our group has previously conducted in-depth studies on the ability of GREM1 knockdown to promote the osteogenic differentiation of MSCs, and the ability of GREM1 overexpression to inhibit their osteogenic differentiation; however, to date, no experiments have confirmed the regulatory effect of GREM1 on the osteogenic differentiation of DPSCs in vivo. Therefore, we conducted subcutaneous implantation experiments in nude mice, and HE staining and immunohistochemical staining confirmed that knockdown of GREM1 promoted osteo-/dentinogenic differentiation of DPSCs in vivo. To explore the regula-

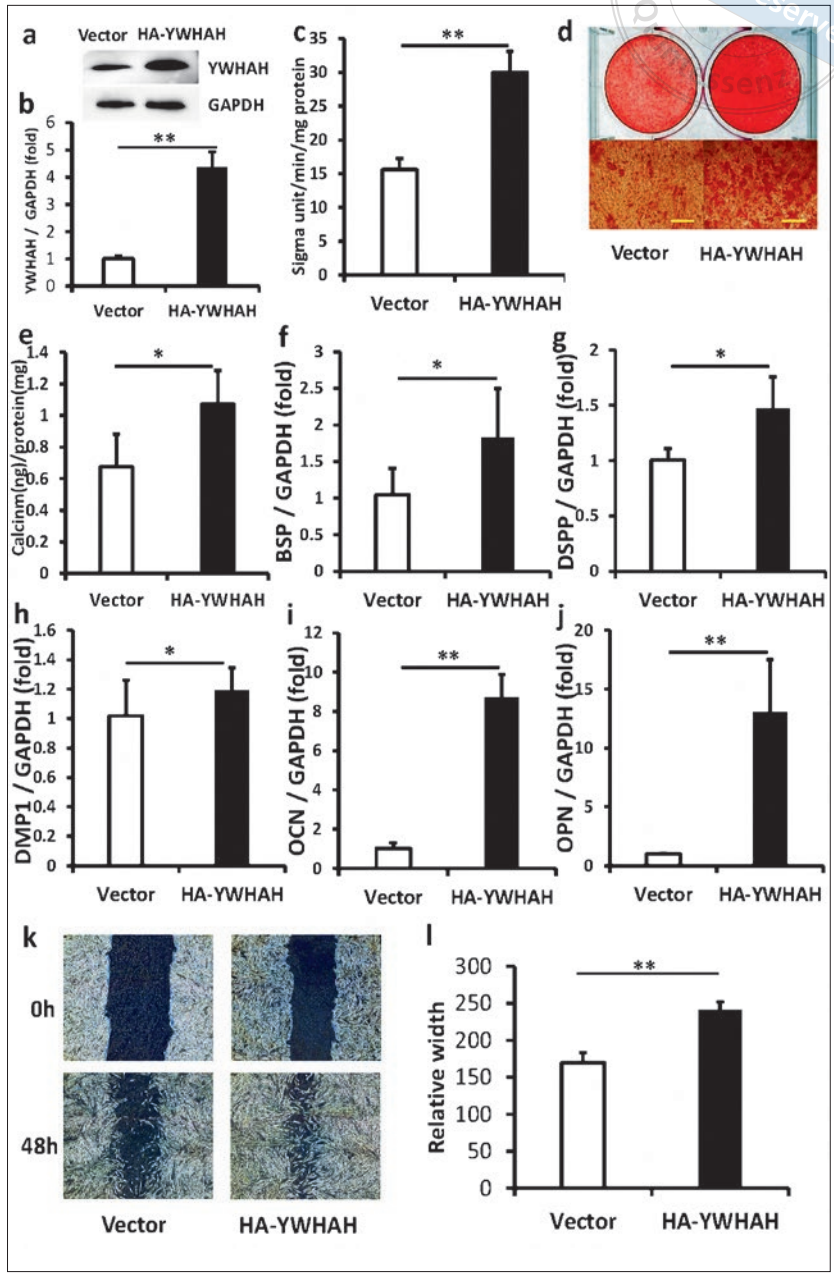

Fig 6a to l Overexpression of YWHAH promoted the osteo-/dentinogenic differentiation of DPSCs in vitro. Western blot showing YWHAH expression **(a)**. Real-time RT-PCR showed the overexpression efficiency of YWHAH in DPSCs **(b)**. ALP activity assay **(c)**. Alizarin red staining **(d)**. Quantitative calcium analysis **(e)**. The expression of DSPP **(f)**, DMP1 **(g)** and BSP **(h)**, OPN **(i)** and OCN **(j)** was detected by real-time RT-PCR at 14 days after induction. The result of scratch-simulated wound migration assay **(k and l)**. GAPDH was used as an internal control. A Student *t* test was performed to determine statistical significance. All error bars represent the standard deviation (n = 6). *$P \leq 0.05$, **$P \leq 0.01$.

tory mechanism of GREM1, we performed a co-IP assay and found that GREM1 can bind to YWHAH in DPSCs. Functional verification revealed that YWHAH knockdown suppressed the osteo-/dentinogenesis of DPSCs in vitro, whereas YWHAH overexpression promoted the osteo-/dentinogenesis of DPSCs in vitro. The product of the YWHAH gene is the 14-3-3 eta protein.[25-27] The 14-3-3 proteins are a family of conserved regulatory molecules expressed in all eukaryotic cells. A striking feature of these proteins is their ability to bind a multitude of functionally diverse signaling proteins, including kinases, phosphatases and transmembrane receptors.[28,29] This plethora of interacting proteins allows 14-3-3 to play important roles in a wide range of vital regulatory processes, such as mitogenic signal transduction, apoptotic cell death and cell cycle control.[30,31] Acronyms14-3-3 family proteins interact with many signalling molecules, such as MAPK kinase, Raf-1, Wee1, Cdc25, cyclin B1, protein kinase C, IGF-I receptor, insulin receptor substrate 1, Bad and Bcl, and regulate several signal transduction pathways. Additionally, 14-3-3 proteins help two molecules interact or interrupt the association between

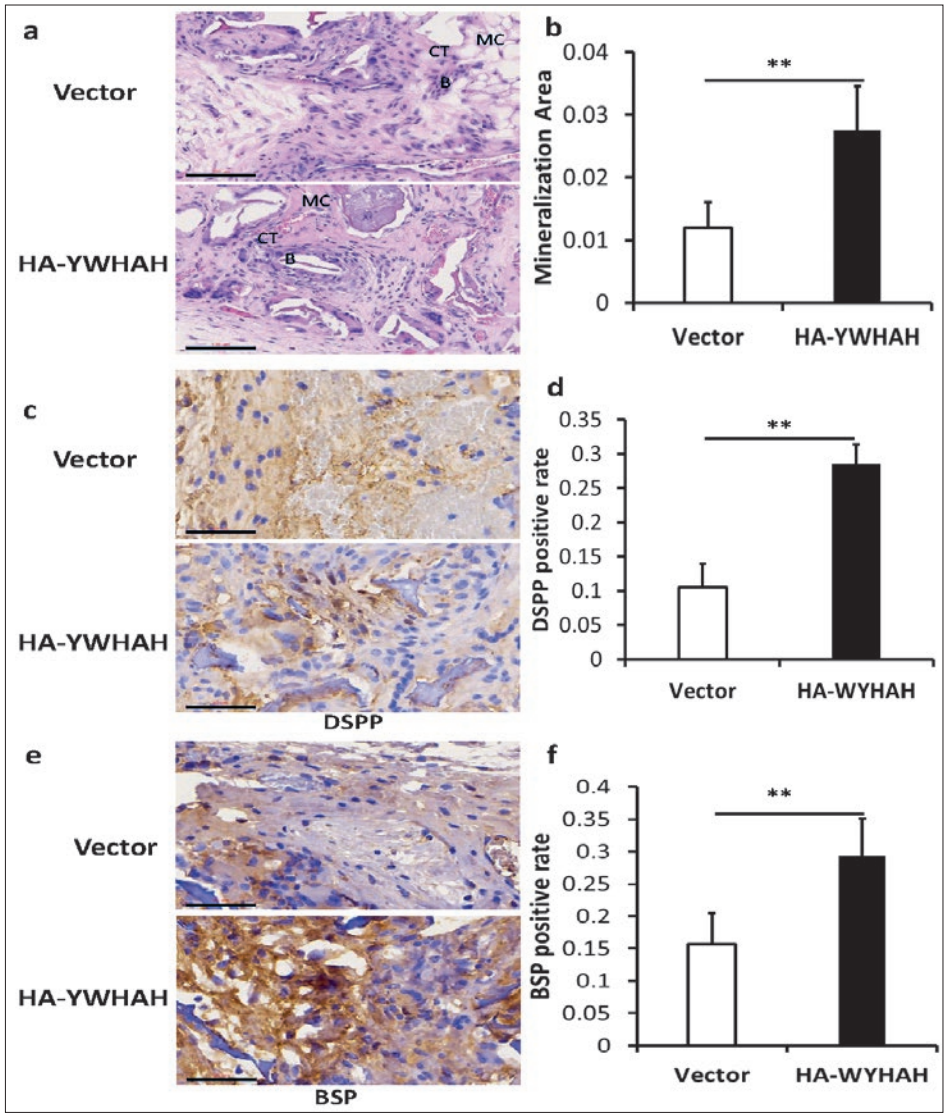

Fig 7a to f Overexpression of YWHAH promoted the osteo-/dentinogenic differentiation of DPSCs in vivo. HE staining results showing bone/dentine-like tissue formation. Scale bar 100 μm. B, bone/dentine-like tissues; CT, connective tissue; MC, mineral collagen **(a)**. Quantitative measurement of the HE staining results **(b)**. Immunohistochemical staining and quantitative analysis of DSPP **(c and d)**. Immunohistochemical staining and quantitative analysis of BSP. Scale bar: 50 μm **(e and f)**. A Student *t* test was performed to determine statistical significance. All error bars represent the standard deviation (n = 6). $*P \leq 0.05$, $**P \leq 0.01$.

them by functioning as molecular scaffolds.[32] However, the effect of YWHAH on osteogenic differentiation of dental stem cells is still unclear, and the present study demonstrated for the first time the ability of YWHAH to promote the differentiation of dental pulp stem cells. Through the above experiments, we suggest that YWHAH might be an important downstream gene of GREM1 that regulates BMP expression and stem cell function. In the future, we will conduct further research on the GREM1-YWHWH complex interaction and the effect of small molecule polypeptides on the differentiation of DPSCs to lay a foundation for the application of small molecule preparations in root regeneration and clinical practice.

Conclusion

In conclusion, the present findings highlight the key role played by GREM1 in osteo-/dentinogenic differentiation of DPSCs, which may be a potential target gene for promoting MSC osteo-/dentinogenic differentiation and tissue regeneration.

Conflicts of interest

The authors declare no conflicts of interest related to this study.

Author contribution

Drs Shu DIAO, Xiao HAN, Wei Long YE, Chen ZHANG and Dong Mei YANG contributed to the material preparation, data collection and analysis; Dr Shu DIAO drafted the manuscript and all authors contributed comments; Profs Zhi Peng FAN and Song Ling WANG contributed to the study conception and design. All authors read and approved the final manuscript.

(Received Nov 18, 2023, accepted April 08, 2024)

References

1. Liu Y, Zheng Y, Ding G, et al. Periodontal ligament stem cell-mediated treatment for periodontitis in miniature swine. Stem Cells 2008;26:1065–1073.
2. Ding G, Liu Y, Wang W, et al. Allogeneic periodontal ligament stem cell therapy for periodontitis in swine. Stem Cells 2010;28:1829–1838.
3. Li D, Wang X, Yao L, et al. Sox2 controls asymmetric patterning of ameloblast lineage commitment by regulation of FGF signaling in the mouse incisor. J Mol Histol 2021;52:1035–1042.
4. Nireeksha, Varma SR, Damdoum M, et al. Immunomodulatory Expression of Cathelicidins Peptides in Pulp Inflammation and Regeneration: An Update. Curr Issues Mol Biol 2021;43:116–126.
5. Cho YD, Kim KH, Lee YM, Ku Y, Seol YJ. Dental-derived cells for regenerative medicine: stem cells, cell reprogramming, and transdifferentiation. J Periodontal Implant Sci 2022;52:437–454.
6. Diao S, Lin X, Wang L, et al. Analysis of gene expression profiles of apical papilla tissues, stem cells from apical papilla and cell sheet. Cell Prolif 2017;50:e12337.
7. Diao S, Yang H, Cao Y, Yang D, Fan Z. IGF2 enhanced the osteo-/dentinogenic and neurogenic differentiation potentials of stem cells from apical papilla. J Oral Rehabil 2020;47(suppl 1):55–65.
8. Canalis E, Parker K, Zanotti S. Gremlin1 is required for skeletal development and postnatal skeletal homeostasis. J Cell Physiol 2012;227:269–277.
9. Lovely AM, Duerr TJ, Qiu Q, Galvan S, Voss SR, Monaghan JR. Wnt Signaling Coordinates the Expression of Limb Patterning Genes During Axolotl Forelimb Development and Regeneration. Front Cell Dev Biol 2022;10:814250.
10. Church RH, Krishnakumar A, Urbanek A, et al. Gremlin1 preferentially binds to bone morphogenetic protein-2 (BMP-2) and BMP-4 over BMP-7. Biochem J 2015;466:55–68.
11. Liu H, Han X, Yang H, et al. GREM1 inhibits osteogenic differentiation, senescence and BMP transcription of adipose-derived stem cells. Connect Tissue Res 2021;62:325–336.
12. Namkoong H, Shin SM, Kim HK, et al. The bone morphogenetic protein antagonist gremlin 1 is overexpressed in human cancers and interacts with YWHAH protein. BMC Cancer 2006;6:74.
13. Hein MY, Hubner NC, Poser I, et al. A human interactome in three quantitative dimensions organized by stoichiometries and abundances. Cell 2015;163:712–723.
14. Liu Z, Hayashi H, Matsumura K, et al. Hyperglycaemia induces metabolic reprogramming into a glycolytic phenotype and promotes epithelial-mesenchymal transitions via YAP/TAZ-Hedgehog signalling axis in pancreatic cancer. Br J Cancer 2023;128:844–856.
15. Uemura M, Nagasawa A, Terai K. Yap/Taz transcriptional activity in endothelial cells promotes intramembranous ossification via the BMP pathway. Sci Rep 2016;6:27473.
16. Wang H, Yu H, Huang T, Wang B, Xiang L. Hippo-YAP/TAZ signaling in osteogenesis and macrophage polarization: Therapeutic implications in bone defect repair. Genes Dis 2023;10:2528–2539.
17. Pan H, Xie Y, Zhang Z, et al. YAP-mediated mechanotransduction regulates osteogenic and adipogenic differentiation of BMSCs on hierarchical structure. Colloids Surf B Biointerfaces 2017;152:344–353.
18. Yang H, Cao Y, Zhang J, et al. DLX5 and HOXC8 enhance the chondrogenic differentiation potential of stem cells from apical papilla via LINC01013. Stem Cell Res Ther 2020;11:271.
19. Gu Q, Luo Y, Chen C, Jiang D, Huang Q, Wang X. GREM1 overexpression inhibits proliferation, migration and angiogenesis of osteosarcoma. Exp Cell Res 2019;384:111619.
20. Guan Y, Cheng W, Zou C, Wang T, Cao Z. Gremlin1 promotes carcinogenesis of glioma in vitro. Clin Exp Pharmacol Physiol 2017;44:244–256.
21. Pérez-Lozano ML, Sudre L, van Eegher S, et al. Gremlin-1 and BMP-4 Overexpressed in Osteoarthritis Drive an Osteochondral-Remodeling Program in Osteoblasts and Hypertrophic Chondrocytes. Int J Mol Sci 2022;23:2084.
22. O'Reilly S. Gremlin: a complex molecule regulating wound healing and fibrosis. Cell Mol Life Sci 2021;78:7917–7923.
23. Jang BG, Kim HS, Chang WY, et al. Prognostic significance of stromal GREM1 expression in colorectal cancer. Hum Pathol 2017;62:56–65.
24. Kim HS, Shin MS, Cheon MS, et al. GREM1 is expressed in the cancer-associated myofibroblasts of basal cell carcinomas. PLoS One 2017;12:e0174565.
25. Navarrete M, Zhou Y. The 14-3-3 Protein Family and Schizophrenia. Front Mol Neurosci 2022;15:857495.
26. Huang X, Zheng Z, Wu Y, Gao M, Su Z, Huang Y. 14-3-3 Proteins are Potential Regulators of Liquid-Liquid Phase Separation. Cell Biochem Biophys 2022;80:277–293.
27. Guo M, He M, Zhang Y, et al. Nucleo-cytoplasmic shuttling of 14-3-3 epsilon carrying hnRNP C promotes autophagy. Cancer Biol Ther 2023;24:2246203.
28. Morrison DK. The 14-3-3 proteins: integrators of diverse signaling cues that impact cell fate and cancer development. Trends in Cell Biol 2009;19:16–23.
29. Lu YC, Cheng AJ, Lee LY, et al. MiR-520b as a novel molecular target for suppressing stemness phenotype of head-neck cancer by inhibiting CD44. Sci Rep 2017;7:2042.
30. Haonon O, Rucksaken R, Pinlaor P, et al. Upregulation of 14-3-3 eta in chronic liver fluke infection is a potential diagnostic marker of cholangiocarcinoma. Proteomics Clin Appl 2016;10:248–256.
31. Ren L, Li Y, Zhao Q, et al. miR-519 regulates the proliferation of breast cancer cells via targeting human antigen R. Oncol Lett 2020;19:1567–1576.
32. Zhou Y, Liu S, Luo Y, Zhang M, Jiang X, Xiong Y. IncRNA MAPKAPK5-AS1 promotes proliferation and migration of thyroid cancer cell lines by targeting miR-519e-5p/YWHAH. Eur J Histochem 2020;64:3177.